Simultaneous Depth-Profiling of Electrical and Elemental Properties of Ion-Implanted Arsenic in Silicon by Combining Secondary-Ion Mass Spectrometry with Resistivity Measurements

N. S. Bennett *[#], C. S. Wong [%] and P. J. McNally

Nanomaterials Processing Lab., School of Electronic Engineering, Dublin City University, Dublin 9, Ireland

* Email N.Bennett@hw.ac.uk, Tel. +44 131 451 4379, Fax +44 131 451 3129

[#] Now at Nano-Materials Lab., School of Engineering and Physical Sciences, Heriot-Watt University, Edinburgh EH14 4AS, United Kingdom

[%] Now at Sonex Metrology Ltd., Swords Enterprise Park, Swords, Co. Dublin, Ireland

A method is proposed to extract the electrical data for surface doping profiles of semiconductors in unison with the chemical profile acquired by secondary-ion mass spectrometry (SIMS) – a method we call SIMSAR (secondary-ion mass spectrometry and resistivity). The SIMSAR approach utilizes the inherent sputtering process of SIMS, combined with sequential four-point van der Pauw resistivity measurements, to surmise the active doping profile as a function of depth. The technique is demonstrated for the case of ion-implanted arsenic doping profiles in silicon. Complications of the method are identified, explained and corrections for these are given. While several techniques already exist for chemical dopant profiling and numerous for electrical profiling, since there is no technique which can measure both electrical and chemical profiles in parallel, SIMSAR has significant promise as an extension of the conventional dynamic SIMS technique, particularly for applications in the semiconductor industry.

Introduction

Secondary-ion mass spectrometry (SIMS) is an established technique for measuring doping profiles in semiconductors. The method benefits from high sensitivity, wide dynamic range and good depth resolution [1]. These advantages have made it a staple technique in the semiconductor industry for measuring the one-dimensional depth-profile of ion-implanted dopants – such as arsenic – in silicon. One limitation of the SIMS technique is that while it identifies the total concentration of an element as a function of depth, it is unable to distinguish between atoms that act as donors or acceptors from those that do not, i.e. it cannot distinguish so-called 'active' dopants from 'inactive' dopants. The lack of electrical information is also a feature of some other, less common, methods of elemental dopant depth-profiling, such as medium-energy ion scattering [2], high-resolution Rutherford back-scattering [3] and atom probe tomography [4]. This is an increasingly important limitation for the semiconductor industry in particular, as chipmakers employ ever higher doping concentrations in cutting-edge silicon devices. Many of these concentrations are in excess of dopant solid-solubility levels, meaning large portions of ion-implanted dopants do not occupy substitutional lattice sites, but instead are interstitial in the host lattice, usually in the form of clusters. A number of electrical measurement techniques exist that can accurately determine the active dopant profile as a function of depth, such as spreading-resistance based techniques, for example scanning spreading resistance measurements (SSRM) [5] or spreading resistance profiling (SRP) [6]. Spreading-resistance tools offer excellent depth and spatial resolution. Other techniques used for electrical profiling include capacitance-voltage (CV) measurements [7], scanning capacitance measurements (SCM) [8], differential Hall measurements (DHM) [9] and resistivity depth-profiling (RDP) [10]. All of these electrical methods are complementary to SIMS measurements, but currently they must be carried out separately. This brings the disadvantage that a minimum of two pieces of expensive equipment are required for comprehensive characterisation, in addition to the obvious drawbacks of carrying out measurements at different times/locations, with diverse sample geometries or on completely different samples. Fig. 1 provides an example of the difference in the dopant depth-profile of the very same sample measured, in this case, by both SIMS and DHM. Note that both techniques have provided accurate results, the difference being that DHM is only sensitive to arsenic atoms that contribute as donors, whereas SIMS measures the presence of the arsenic atom indiscriminately of whether it is active or otherwise. Fig. 1 highlights why it is so important to know both the elemental and active doping concentration. The active dopant peak in Fig. 1 is an order of magnitude less than the chemical peak revealed by SIMS, i.e. a large proportion of dopant atoms are not contributing electrically. Both of the profiles give vital information, since knowing the electrical activity is key to understanding how the silicon device will perform. Likewise, knowledge of the chemical composition in doped regions is important in order to determine defect concentrations, strain, and material phase. As outlined above, several techniques exist for chemical dopant profiling and numerous for electrical profiling. Crucially however, there is no technique which can measure both electrical and chemical profiles in parallel.

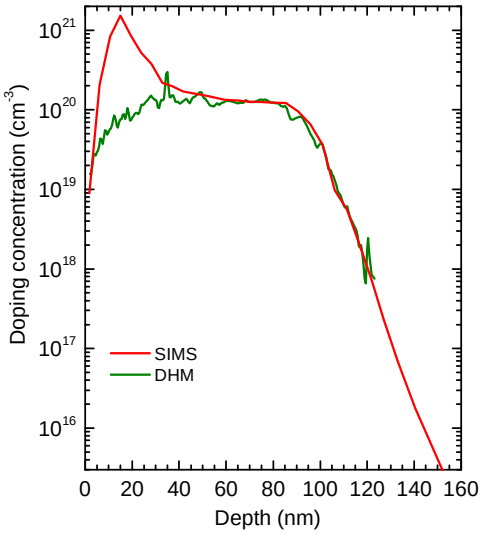

Fig. 1. A comparison of the measured doping profile for As-implanted Si (energy = 80 keV, fluence = 2x10^{15} cm^{-2}) after annealing (900 °C, 180 s) measured by both secondary-ion mass spectrometry (SIMS) (6 keV Cs) and differential Hall measurement (DHM).

Measurement Design

In this article a method is described that allows measurement of the electrically active dopant profile in unison with the chemical profile. Since SIMS is the routinely-used technique of the semiconductor industry, we propose a method to extract electrical dopant data alongside the elemental depth-profiling acquired by SIMS. This is hereon referred to as SIMSAR (secondary-ion mass spectrometry and resistivity). The SIMSAR approach utilizes the inherent sputtering process of SIMS, combined with sequential four-point van der Pauw resistivity measurements, to infer the active doping profile as a function of depth. The method is not without complications, however potential problems are identified, explained and corrections for these are outlined in the article. The measurement principle is tested to the point where it could feasibly be developed for incorporation into a commercial SIMS tool for use in semiconductor manufacturing metrology.

The electrical measurements of SIMSAR are based on the process of differential sheet resistance profiling as has been demonstrated using micro-four-point-probe [11], and as part of the DHM process. In the former case, a beveled sample is used for depth-profiling, and in the latter, (electro-) chemical etching of the central portion of a cloverleaf- or 'Greek cross'-shaped sample is used. Both approaches are incompatible with SIMS in its current form. However, it is the DHM approach which we have modified in order to give compatibility with SIMS. This required two distinct steps: (i) modification of the effective sample size, and (ii) alteration of the 'etch' procedure:

i. Resistivity measurements were first carried out with the same sample geometry that is often used for differential Hall profiling (Fig. 2), i.e. sample scale of 1 cm by 1 cm. Of this, the central 1 mm x 1 mm is effectively the sample (dotted-line in Fig. 2), with four 'arms' acting as edge contacts. In DHM, only this central 1 mm^2 square is subjected to the etch process for depth-profiling. During SIMS analysis a small sputtered square is probed, with sample area of the

order of 50 µm x 50 µm. Therefore the normal sample sizes of the two techniques are at odds, and a reduction in the central square for the electrical measurement was required to bring it below the size of the SIMS sputter area (blue zone in Fig. 2).

ii. Secondly, for compatibility with SIMS, the layer removal process was not done using chemical etching. Instead we have utilized sputtering for layer removal.

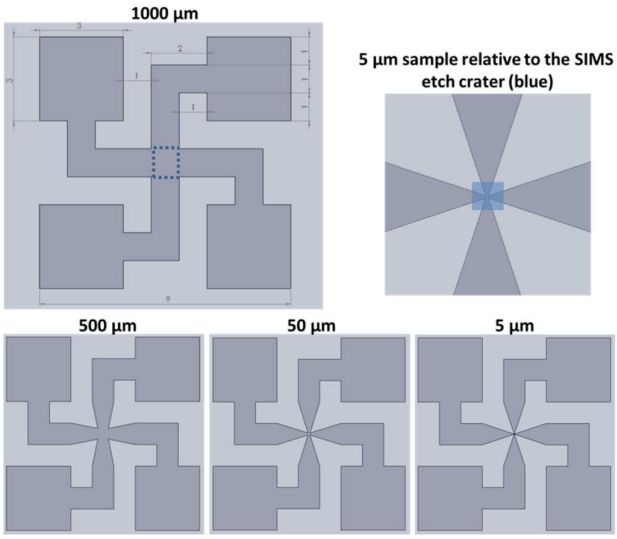

Fig. 2. Ordinary sample geometry used for differential resistivity/Hall profiling (top-left) showing sample dimensions in mm (gray inset). The central portion (illustrated by dotted-line) acts as the 'effective sample', while the four 'arms' act as edge contacts to the central square (1000 µm-diameter). The 'effective sample' size can be varied sequentially down to 5 µm – making it less than the size of a typical SIMS etch-crater (blue-shading in top-right). Note that the lighter grey region represents an area that has been mesa etched.

Experimental Details

Test samples were created from 100 mm diameter, <100> silicon wafers (p-type, 10 – 20 Ωcm). Doping was introduced by ion-implantation of arsenic (energy 80 keV or 150 keV / fluence $2x10^{15}$ cm^{-2} or 10^{15} cm^{-2}). Wafers were annealed at 900 °C for 180 s in nitrogen. Photolithography and etching were used to define 9 mm cross patterns on each wafer, with the central square of each cross being one of eight different diameters – 1000 µm, 500 µm, 300 µm, 100 µm, 50 µm, 30 µm, 10 µm or 5 µm (Fig. 2). Wafers were then diced into 1 cm x 1 cm pieces, each with a single cross pattern. Van der Pauw resistance and Hall measurements were carried out on a number of samples to confirm non-variability from sample-to-sample using a RH6000 Hall measurement tool. A maximum difference of only 4% was recorded, equal in magnitude to the uncertainty in the measurement technique. Although reduction of the central square to single micrometer diameters should not compromise the validity of the van der Pauw principle [12], tests were carried out to confirm this. The results are summarized in Fig. 3 which shows the mean sheet resistance and mean Hall coefficient as a function of sample size. The spread of both quantities was less than 4% and no systematic variation with sample size was observed.

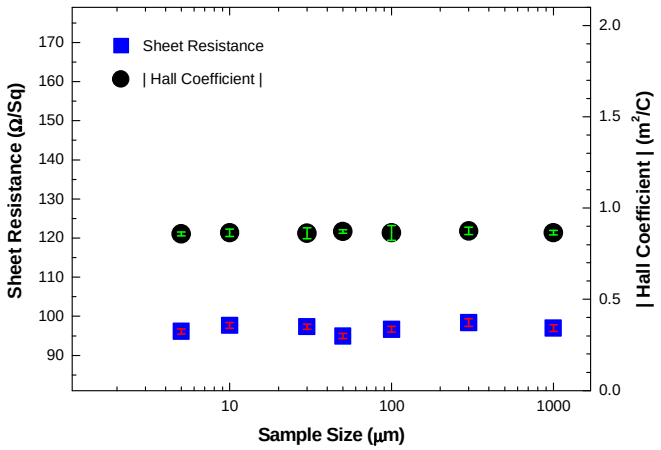

Fig. 3. Hall coefficient and sheet resistance measurements for As-implanted Si (150 keV, 10^{15} cm^{-2}) after annealing (900 °C, 180 s), showing no systematic variation was evident as a function of sample size. Error bars indicate the sample-to-sample variation of different samples of the same diameter.

To further characterize these samples prior to investigation by SIMSAR measurement, several cross-shaped samples were measured by differential Hall on a Biorad HL5900 tool using chemical etching [9]. This measurement allowed doping concentrations to be extracted in two ways. Firstly, from measured Hall coefficient data and secondly via differential resistivity measurements, where doping concentrations were extracted from conversion of the measured resistivity values in a similar way as for SRP data analysis [13]. All of these electrical measurements are presented in Figure 4 alongside SIMS and are in reasonably close agreement with one another. For total doping concentrations $<10^{20}$ cm^{-3}, such as in the tail of the doping profile, as well as being in good agreement with each other, electrical measurements are also in reasonable agreement with SIMS. For doping concentrations $>10^{20}$ cm^{-3} the agreement with SIMS is poor, for reasons outlined in the *Introduction* section. This range of electrical doping measurements act as a means of comparison for subsequent data extracted using the sputtering-based SIMSAR approach.

SIMS was carried out at a pressure of 10^{-5} Pa on the 5 μm samples using a Cameca SC Ultra system using a low-energy Cs beam to extract elemental doping profiles. Initially a 6 keV ion beam was used, however this was lowered to 2 keV and then to 0.8 keV for reasons that will be explained later. A square SIMS etch crater of 30 μm x 30 μm was created during sputtering and was created to coincide with the sample center as illustrated in Figure 2 (top-right). Of this sputtered area, only secondary-ions collected from the central 5 μm x 5 μm were counted towards the depth-profile to avoid contamination from crater walls. To allow resistivity information to be recorded in parallel, only a small modification to the sample mounting procedure was necessary. Samples were secured on the mounting stage of the SIMS tool as for a regular depth profile measurement, held in place using a plastic pin. Additionally, a metallic pin was placed on each of the mesa arms (four in total), and connected via feed-through to a Keithley current source (Model 6221) and multimeter (Model 2700), external to the chamber. The electrical measurement apparatus was controlled by a LabView program running on a separate PC and was set to eliminate the floating potential of the stage from all measured potential differences recorded between two corners of a sample, when a current was injected between the other two. During the SIMS measurements, the four-point van der Pauw resistance [12]

was measured and recorded every 10 seconds. The measured resistance values were converted into a resistivity depth profile. Since the incident ion beam continued to sputter during the electrical measurement, strictly the measurement depth was varying during the measurement. However, since an etch rate of ~0.5 nm s^{-1} was used, the impact of this change was negligible. The etch rate was determined by measuring the total crater depth by atomic-force microscopy after the SIMSAR experiment had finished.

In order to determine the charge-carrier depth profile from the raw measurement data the following calculations were performed: First the sheet resistance of the layer removed during the nth etching step (ΔR_n) was calculated from the sheet resistance before (R_n) and after (R_{n+1}) the nth etching step:

$$\Delta R_n = \frac{R_{n+1}.R_n}{R_{n+1} - R_n} \quad (1)$$

where R_n refers to the sheet resistance measured at depth d_n and R_{n+1} is the sheet resistance at depth d_{n+1}. Then ΔR_n was converted into a resistivity (ρ_n) assuming that the resistivity was a constant across the depth range from d_n to d_{n+1}:

$$\rho_n = (d_{n+1} - d_n).\Delta R_n \quad (2)$$

Finally, resistivity was converted into a carrier concentration using standard conversion tables for As-doped Si [13]. This process, taken for all measured data points, provided a carrier depth-profile that could be plotted alongside the elemental depth-profile acquired from the SIMS process.

Results

In addition to the SIMS, DHM and RDP depth-profiles already described, Figure 4 also shows an electrical depth-profile acquired by the SIMSAR approach. Both 'raw' and 'corrected' plots are presented. Note that the procedure and need for correction will be explained later. In all cases the plots are normalized to a 'zero depth' corresponding to the Si surface, not the wafer surface, which in all cases had a native oxide of between 1.5nm and 2.5nm. This was monitored by measuring the oxygen SIMS signal and the depth-profiles normalized accordingly. It is worth also noting that all measurements were repeated on several samples with excellent reproducibility. Therefore accepting the raw SIMSAR plot in Figure 4 as representative, a comparison with DHM and RDP profiles can be made. Firstly, one can see that the peak carrier concentration measured by all three electrical techniques is in very good agreement. A clear advantage of the SIMSAR method of depth-profiling is that it can measure much deeper in the profile due to a more uniform etch procedure. In the RDP method the data becomes typically unreliable after ~100nm [14]. During the DHM depth-profile, reliability is compromised beyond ~120 nm [14]. The SIMSAR approach remains reliable in accordance with the SIMS measurement and enables electrical measurements right down to the n/p junction (~140 nm). As well as the obvious advantage of the SIMSAR approach, that electrical data and chemical composition are acquired at the same time and at the same sample location, the SIMSAR method also has a shorter measurement time than the other two methods.

In contrast, there are issues with the SIMSAR approach that must be considered and corrected for. The first is the depth resolution. Since electrical measurements were made at 10 s intervals, a corresponding depth resolution of ~5 nm was derived given a ~0.5 nm s^{-1} sputter rate. The resolution can therefore be improved by either (i) increasing the frequency at which measurements are made,

by (ii) reducing the sputter rate, or by a combination of both factors. For a very low beam energy (<1 keV) a depth resolution better than 1 nm was found to be possible [15]. Two other issues are apparent when one inspects the raw SIMSAR plot with respect to DHM or RDP profiles. The first is that the depth profile appears to be shifted towards the surface. This is most evident in the tail of the doping profile where a ~5 nm shift towards the sample surface is apparent. The other discrepancy is at the sample surface, where the raw SIMSAR data is higher in the first 10 nm than any of the other electrical depth-profiles, and higher than even the SIMS profile in the first 5 nm. Both of these discrepancies in the SIMSAR approach are discussed and corrected for in the subsequent section.

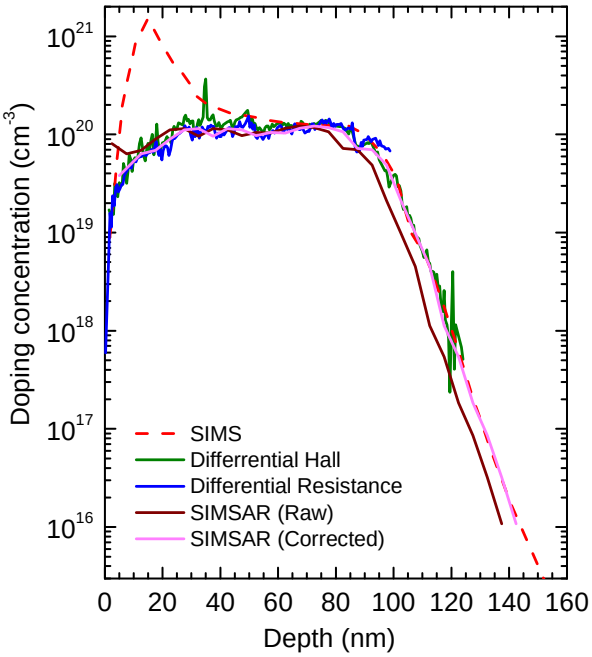

Fig. 4. A comparison of the measured doping profile for As-implanted Si (80 keV, 2x10^{15} cm^{-2}) after annealing (900 °C, 180 s) measured by secondary-ion mass spectrometry (SIMS) (6 keV Cs), differential Hall, differential resistance, and SIMSAR (both corrected and uncorrected).

Discussion

The two issues identified in the SIMSAR depth-profile can be explained by the same feature of the measurement technique. The artificially high electrical activation at the surface is caused by an issue with the first measured data point. It is a result of the damage caused to the sub-surface immediately beneath the part of the sample that has been most recently sputtered – see Figure 5(a). Essentially, the first measurement is made before sputtering has started (point 0) and therefore that resistance measurement is representative of electrical properties of the whole doped layer. During sputtering, after 5 nm of material is removed, a second resistance measurement is made. From equation (1), the sheet resistance and resistivity of the removed layer is calculated – via equations (1) and (2) – under the assumption that $d_1 - d_0$ (the removed depth) is 5 nm. The problem arises because immediately below the sputtered surface a 'mixing' layer of damaged Si is created, caused by the ion cascade of the incident SIMS beam. The damaged layer does not contribute to the electrical measurement, effectively removing part of the doped region from the second measurement. According to equations (1) and (2), a disproportionate increase in resistance is recorded by the effective removal of a region greater than 5 nm thick, hence why the dopant concentration for this data point is over-estimated.

This is illustrated in Figure 5(b). Theoretically, the first data point should be placed at a depth midway between surface 0 and surface 1, but in reality, the difference between surface 0 and 'effective' surface 1 is greater. Figure 5(b) also demonstrates why this factor is only encountered for the first data point, as providing the sputter conditions remain the same, the extent of the mixing layer between the etch crater is present and equal for all subsequent measurements, creating no additional impact. The explanation of this feature is supported when comparing the electrical profiles as the Cs beam energy is varied, as in Figure 6. The effect becomes more significant for higher beam energies such as 6 keV, as opposed to 800 eV as the extent of the ion beam-induced damage and mixing-layer becomes greater.

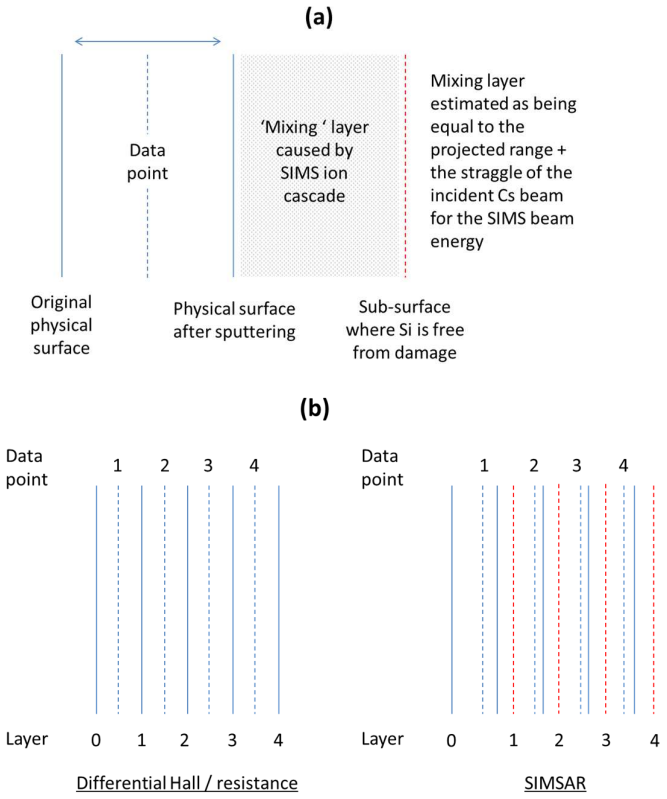

Fig. 5. A schematic illustration of (a) the position and creation of a 'mixing 'layer', which leads to a shift towards the surface of the SIMSAR doping profile, and (b) the depth at which the SIMSAR data points should be plotted.

It is this same mixing-layer phenomenon that is responsible for the surface shift, also shown schematically in Figure 5(b), with the dashed blue lines illustrating the appropriate depth position corresponding to successive data points. In Figure 5(a) (DHM and RDP), the data point is plotted midway between any two layers, whereas in Figure 5(b), SIMSAR data points are plotted deeper than midway. This offset applies to all data points and explains why the SIMSAR raw data plot appears shifted towards the surface.

This mixing-layer effect has been previously identified [16] and can be corrected for by making a straight-forward modification to the data analysis. The most important thing is to correctly identify the depth of the mixing layer. This is dependent on the energy of the incident Cs beam, and can be accurately estimated as being equal to the *projected range + the straggle* of the incident beam [16],

which can be calculated using software such as SRIM or SUSPRE [17-18], and is equally applicable for different SIMS species or different target materials. Corrections to the raw SIMSAR data in Figure 6(a) are applied in Figure 6(b) by adding *projected range + the straggle* to the depth axis. This amends the over-estimated dopant activation in the near surface for each of the three beam energies, as well as correcting the shift towards the surface. This could be further corrected to take account of the variable incident beam angle.

For significantly shallower implants, profile shifts due to the transient nature of the sputter yield may also need to be considered [19].

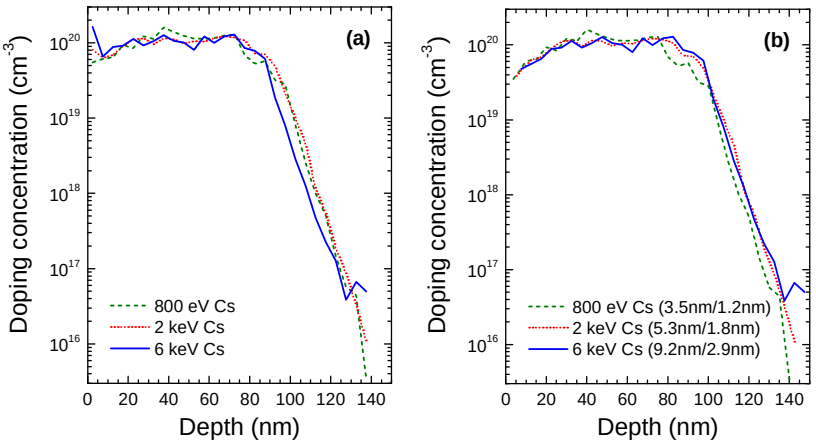

Fig. 6. A comparison of (a) raw data and (b) corrected data for SIMSAR measurements made with various Cs incident ion energies. Values in parentheses are ion projected range/straggle [18].

Outlook

While presently the SIMSAR method has been tested only on arsenic-doped silicon, it is likely to be equally applicable to other dopants, different substrates and for different incident ion beams. In order for the technique to be widely adopted in commercial SIMS tools, the development of a dedicated sample stage for *in situ* electrical measurements would be required, including integration of the electrical measurement control software with the SIMS tool. However this should be relatively straight-forward and such a set-up would be compatible with SIMS tools in their current form.

A complication of the SIMSAR technique is that the sample structure would need to be like that in Fig. 2 (top-right), potentially requiring additional lithographic, etching steps and metal pads for many samples. However, for the semiconductor industry, where fabricated wafers can routinely include square test pads for SIMS measurements, forming cross-shape sample structures instead, is likely to be straight-forward, requiring little, if any, additional processing or cost.

Conclusion

A method was proposed to extract the electrical data for surface doping profiles of semiconductors in unison with the chemical doping profile acquired by secondary-ion mass spectrometry (SIMS) – the so-called SIMSAR technique. The approach utilizes the inherent sputtering process of SIMS, combined with sequential four-point van der Pauw resistivity measurements, to infer the active doping profile

as a function of depth. The technique was demonstrated for the test case of ion-implanted arsenic doping profiles in silicon. Complications of the method were identified, explained and a methodology for corrections to these were described and verified. Numerous electrical depth-profiling techniques exist, but are often faced with the difficulty of achieving a reliable depth scale, something SIMSAR overcomes, as ion beam erosion is very controllable and repeatable versus, say, chemical etching. While several techniques also already exist for chemical dopant profiling, since there is currently no technique which can measure both electrical and chemical profiles in parallel, SIMSAR has significant promise as an extension of the conventional SIMS technique, particularly for applications in the semiconductor industry.

Acknowledgements

This work was fully funded by Science Foundation Ireland grant 11/TIDA/I1971. The authors also acknowledge Ireland's National Access Programme through grant NAP400 for providing facilities for sample fabrication and measurement. We also express our thanks to Prof Russell Gwilliam at the University of Surrey for allowing access to the Biorad HL5900 tool for differential Hall measurements.

References

[1] H. W. Werner, Surf. Interface Anal. **2**(2), 56 (1980)

[2] J. A. Van den Berg, D. G. Armour, S. Zhang, S. Whelan, H. Ohno, T.-S. Wang, A. G. Cullis, E. H. J. Collart, R. D. Goldberg, P. Bailey and T. C. Q. Noakes, J. Vac. Sci. Technol. B **20**, 974 (2002)

[3] C. W. White, S. R. Wilson, B. R. Appleton and F. W. Young Jr., J. Appl. Phys. **51**, 738 (1980)

[4] P. M. Voyles, D. A. Muller, J. L. Grazul, P. H. Citrin and H.-J. L. Gossmann, Nature **416**, 826 (2002)

[5] P. Eyben, M. Xu, N. Duhayon, T. Clarysse, S. Callewaert, and W. Vandervorst, J. Vac. Sci. Technol. B **20,** 471 (2002)

[6] P. De Wolf, T. Clarysse, W. Vandervorst, L. Hellemans, Ph. Niedermann and W. Hänni, J. Vac. Sci. Technol. B **16**, 355 (1998)

[7] Y. Huang and C. C. Williams, J. Vac. Sci. Technol. B **12**, 369 (1994)

[8] C. C. Williams, Annual Review of Materials Science **29**, 471 (1999)

[9] N. S. Bennett, A. J. Smith, B. Colombeau, R. Gwilliam, N. E. B. Cowern, and B. J. Sealy, Mater. Sci. Eng. B **124**, 305 (2005)

[10] D. K. Schroder, "Semiconductor Material and Device Characterization" 3rd Edition, Wiley-Interscience, New York, 2006, p.25

[11] T. Clarysse, P. Eyben, B. Parmentier, B. Van Daele, A. Satta, and W. Vandervorst, J. Vac. Sci. Technol. B **26**, 317 (2008)

[12] L. J. van der Pauw, Philips Res. Repts. **13**, 1-9 (1958)

[13] T. Clarysse, M. Caymax, P. De Wolf, T. Trenkler, W. Vandervorst, J. S. McMurray, J. Kim, C. C. Williams, J. G. Clark, G. Neubauer, J. Vac. Sci. Technol. B **16**, 394 (1998)

[14] HL5900PC Hall Profiler System User Manual 2.0, by Accent Technologies, 2001

[15] L. H. Vanamurthy, M. Huang, H. Bakhru, T. Furukawa, N. Berliner, J. Herman, Z. Zhu, P. Ronsheim, and B. Doris, J. Vac. Sci. Technol. A **31**, 031403 (2013)

[16] W. Vandervorst, H. E. Maes, and R. F. De Keersmaecker, J. Appl. Phys. **56**, 1425 (1984)

[17] J. Ziegler, et al., SRIM - The Stopping and Range of Ions in Matter. May 2009, http://www.srim.org/

[18] R. P. Webb, SUSPRE Version 2.1.3, 2001, http://www.surrey.ac.uk/ati/ibc/research/modelling_simulation/suspre.htm

[19] K. Wittmaack and W. Wach, Nucl. Instr. Meth. **191**(1), 327 (1981)